Active chainmail fabrics for soft robotic applications

2017 Smart Mater. Struct. 26 08LT02

(http://iopscience.iop.org/0964-1726/26/8/08LT02)

OPEN ACCESS
IOP Publishing

Letters
Smart Materials and Structures

Smart Mater. Struct. **26** (2017) 08LT02 (6pp) https://doi.org/10.1088/1361-665X/aa7221

Letter

Active chainmail fabrics for soft robotic applications

Mark Ransley[1,2], Peter Smitham[3,4] and Mark Miodownik[1,5,6]

[1] Mechanical Engineering Department, UCL., London, United Kingdom
[2] CoMPLEX, UCL, London, United Kingdom
[3] Div of Surgery & Interventional Sci, UCL, Royal National Orthopaedic Hospital, United Kingdom
[4] Royal Adelaide Hospital, Adelaide, Australia
[5] Institute of Making, UCL, London, United Kingdom

E-mail: m.miodownik@ucl.ac.uk

Received 22 June 2016, revised 5 May 2017
Accepted for publication 10 May 2017
Published 11 July 2017

Abstract

This paper introduces a novel type of smart textile with electronically responsive flexibility. The chainmail inspired fabric is modelled parametrically and simulated via a rigid body physics framework with an embedded model of temperature controlled actuation. Our model assumes that individual fabric linkages are rigid and deform only through their own actuation, thereby decoupling flexibility from stiffness. A physical prototype of the active fabric is constructed and it is shown that flexibility can be significantly controlled through actuator strains of $\leqslant 10\%$. Applications of these materials to soft-robotics such as dynamically reconfigurable orthoses and splints are discussed.

Supplementary material for this article is available online

Keywords: chainmail, fabric, 3D printing, soft robotics, modelling, controlable

(Some figures may appear in colour only in the online journal)

1. Introduction

Recent years have seen a surge of interest in chainmail fabrics by the design and fashion industries [1]. Additive manufacturing technologies allow for bespoke garments to be printed in one piece from rigid thermoplastics incorporating interlinked parts which yield the meta-properties of flexibility and drape required for garment functionality. Over the same timeframe there has been a corresponding growth in the field of soft robotics. This has been driven by a renewed interest in nature inspired engineering and the recognition that robots based on soft materials have the potential to be more adaptable, robust and safer for human interaction [2]. In this work we bring these two applications together to show that actuated chainmail fabrics have significant potential in soft robotics as well as sectors such as wearable technology, medical devices, aerodynamics, and acoustics [3–5].

1.1. Architectured fabrics

The concept of responsive fabrics is not new but progress has been slow for a number of reasons, the first being the lack of appropriate actuators, and the second being the formidable challenges of manufacturing such an actively interdigitated mechanical system. Engel and Liu [6] fabricated a microscopic chainmail mesh using electroplating techniques, resulting in a material with stretch dependent conductivity. Whilst the mesh was capable of flexing out of plane, the

[6] Author to whom any correspondence should be addressed.

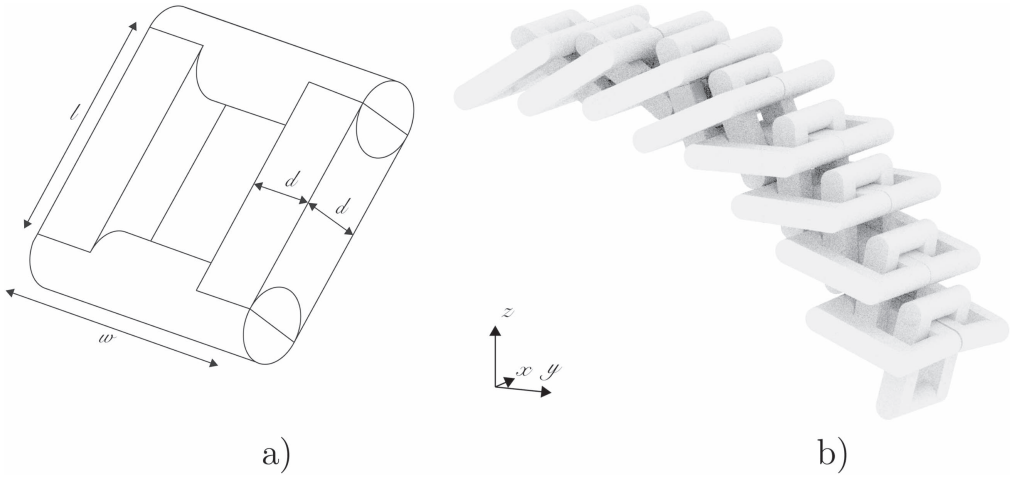

Figure 1. Chainmail structure (a) a single link design showing geometric variables, (b) 8 × 2 chainmail fabric reaching drape equilibrium under the rigid body framework.

researchers only quantified its ability to deform passively through planar stretching and shearing, designing the mesh in such a way that the limits of such deformations could be calculated by inspection.

More recently Rudykh *et al* [7] used a multi-material 3D printer to produce a composite intended for body armour which combined imbricated stiff tiles within a flexible gel matrix where the opposing properties of flexibility and resistance to penetration are balanced optimally. Flexibility of this structure can be programmed as a function of the dimensions and angle of the tiles, however methods of actively modulating this property were not considered.

Henry and McKnight [8] have experimented with laminates containing a combination of constant and variable stiffness elements. In the structural mode, the variable stiffness elements rigidly connect the stiff elements together, creating a stiff structure; in the morphing mode, the variable stiffness material becomes soft leaving the stiff elements effectively disconnected. Henry and McKnight used high yield spring steel as the stiff elements, and shape memory polymer as a variable stiffness actuator in the laminate, but achieved only relatively low maximum strains of 10% with this design, and found the composite had poor toughness, durability and temperature sensitivity. They concluded that this approach showed enormous promise but the current available actuators were unsuitable for large strain structural reconfigurations.

1.2. Concept

The material we have developed solves one of the problems identified by Henry and McKnight [8]: we accommodate the large deformations needed for flexible applications by moving away from laminates and creating a flexible chainmail structure of repeated interlocking links that have two states—closed and open—but also a continuum of intermediate states. The fully closed state when implemented across the fabric renders the material inflexible, essentially creating a stiff material. The open state allows the material to flex along a single axis, as the individual linkages become less closely interlocked. The key to the design is the control of the open and closed states of the individual links, which enables spatial and temporal dynamic control of the structure. Rigid body physics simulations were used to explore the fabric's mechanics and the concept was validated through building a working prototype using a shape memory alloy (SMA), which was integrated into the rigid body framework to produce a hybrid model.

1.3. Actuators

SMAs are biphasic materials exhibiting a transition between the austenite and martensite phases occurring at a critical temperature, Tc, which is accompanied by a shape change. It is this shape change that is ulitised as an actuating force. The most popular SMA, Nitinol (NiTi) is often described as artificial muscle due to its ability deliver large actuating strains and forces [9, 10]. Through annealing NiTi wires into a helical coil the linear strain distance capability can be amplified to arbitrary degrees, though this comes at the cost of linear elasticity across both phases. SMAs generally suffer from functional fatigue whereby the shape memory effect is lost over time, however new alloy design has shown that this can be substantially mitigated [11]. The greatest drawbacks of SMA alloys for active fabrics remains their dependence on temperature changes for actuation and the associated hysteresis.

2. Methods

2.1. Design

The contributions of this paper—namely modulating the fabric's mechanics through embedded SMA actuators, and predicting the mechanics using a rigid body physics framework—are applicable to any fabric design comprising interlinked rigid elements, however in this short communication we present only one example. In this design, each link has

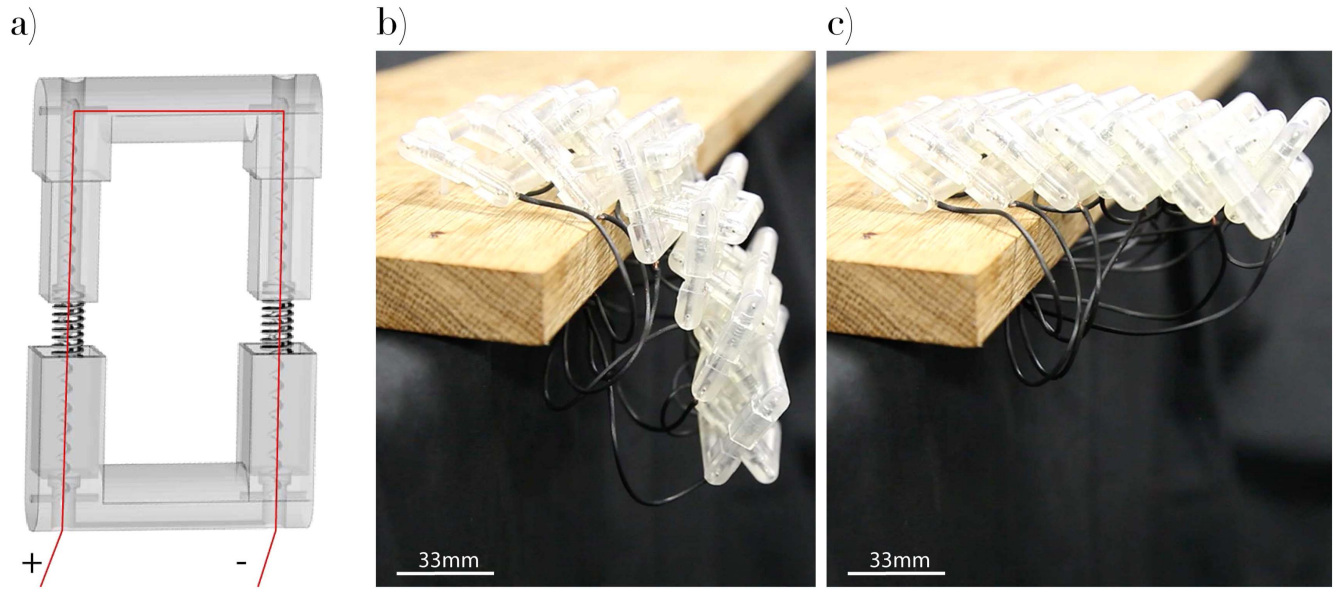

Figure 2. (a) Design of a shape-controlled chainmail linkage where the linear couplings on each side both contain a pair of nested springs, the equilibrium point of which can be adjusted through heating the internal NiTi coils via Joule heating, with charge flowing along the path shown in red. A 6 × 2 physical prototype was fabricated using an SLA 3D printer, and shown to be electronically reconfigurable between flexible (b) and rigid (c) states.

identical geometry and as shown in figure 1(a) its base form is defined by three scalar variables, w, d and l. By aligning the links in an interlocking cartesian array, they form a mesh as shown in figure 1(b), topologically equivalent to the European 4-in-1 (E4-1) chainmail typically found in historic examples [12]. When defining the resolution of an E4-1 mesh, only the links sharing a common orientation are counted, thus the mesh in figure 1(b) has 2 × 8 resolution, despite containing 24 linkages. The width of each link was set according to the mathematical relation $w = 4 * d +$ tol, where tol is the tolerance between the links, held large enough to remove the effects of friction yet sufficiently small as to constrain the linkages' rotation about y and translation across x thus granting the mesh flexibility in the y/z plane only. Alternative designs could be employed to extend the central tenets of this work to control of flexibility across two and three dimensions.

We defined the fabric's flexibility to be the maximum curvature value, $\kappa_{\max}$, obtained whilst bound at one end in a cantilever configuration, where the other end was allowed to flex freely to equilibrium under gravity (figure 1(b)). Curvature in the plane of flexion is defined as

$$\kappa = \frac{|y'z'' - z'y''|}{(y'^2 + z'^2)^{3/2}}. \quad (1)$$

2.2. Fabrication

A physical prototype of the active mesh was realised from the design given in figure 2(a), where a two part linear coupling allowed for linkage deformations corresponding to changes in l (figure 1(a)). Both arms of the linkage contained a paired spring system comprising of a tensile NiTi coil nested within a compressive coil of regular spring steel. The NiTi coils were stretched along the length of the arms and secured in place via steel pins at each end of the linkage chassis, while the compressive coils were secured via cylindrical recesses in the linear coupling. The pins at the top end were sufficiently long as to connect in the centre, forming the circuit highlighted in red in figure 2(a) and allowing for the NiTi spring constant (and thus the linkage parameter l) to be physically modulated via Joule heating. Recesses were calibrated so $l = 3.3$ cm in the cooled state and $l = 3.0$ when heated, corresponding to a 10% strain in the actuators and providing a geometric transformation that initial simulations indicated sufficient to shift the fabric between flexible and rigid states.

The linkage chassis were fabricated in clear resin using a Formlabs Form 2 stereolithography 3D printer, while the NiTi springs were obtained from orthodontics supplier Azdent Dental Corporation. Each linkage was weighed to have mass 7.3 g. A 2 × 6 mesh was assembled and connected to a 6 V power supply, with the three linkages comprising each row connected (36 coils in total) in serial each receiving 1 V. The resistance of an individual coil was measured to be 2.2 Ω with each coil using 454 mA. The total current drawn was 2.72 A, which is equivalent to 16.36 W power supplied to the system.

2.3. NiTi model

To understand the NiTi coil's behaviour as an actuator, a single coil was suspended vertically in a water bath whilst supporting a 500 g mass from below. The water temperature was gradually cycled between 30 °C (fully martensite) and 70 °C (fully austenite), and the coil extension measured at intervals of 2 °C to determine the effect of temperature, T, on the coil's effective spring constant, k. The data displayed the hysteresis curve typical of NiTi actuation, which was then modelled with a dual-Gompertz curve and fitted via

nonlinear-least-squares-regression to yield:

$$k(T) = a\mathrm{e}^{-b\mathrm{e}^{-cT}} + d, \tag{2}$$

where $a, b, c, d = \{0.2305, 17443, 0.1669, 0.1571\}$ for T increasing and $\{0.1996, 696.0, 0.1549, 0.1579\}$ for T decreasing, with residual norm $||r||_2^2 = 0.0058$.

To model the time (t) dependent effect of voltage (U) on the NiTi coil's temperature we used the method from Holschuh *et al* [10]:

$$T(t) = \frac{U^2}{hAR}(1 - \mathrm{e}^{\frac{-hA}{\rho V c_p}t}) + T_\mathrm{a}, \tag{3}$$

where A is the coil's surface area, V its volume, and R its resistance, c_p is the specific heat of NiTi, h its convective heat transfer coefficient and ρ its density, and T_a the ambient temperature. This model neglects the effects of heat transfer via radiation and the $\leqslant$5% contraction in length that NiTi wires exhibit during activation, and assumes $R(t)$ is constant. R was measured to be 2.2 Ω and we calculated $A = 97.85\ \mathrm{mm}^2$ and $V = 7.328\ \mathrm{mm}^3$, whilst $h = 9 \times 10^{-5}\ \mathrm{W\ mm^{-2}\ ^\circ C^{-1}}$, $\rho = 6.45 \times 10^{-3}\ \mathrm{g\ mm^{-3}}$ and $c_p = 0.837\ \mathrm{J\ g^{-1}\ ^\circ C^{-1}}$ were taken from Song *et al* [13].

Letting $t \to \infty$ in (3) yields the maximum temperature obtained for a given voltage:

$$T_\infty = \frac{U^2}{hAR} + T_\mathrm{a}. \tag{4}$$

The heating model was validated by heating and then cooling a single NiTi coil across a range of voltages while the temperature was observed with a Jenoptik VarioCam HD infra-red camera. Average pixel temperature within the coil was computed for each time instance and can be seen to agree with the model (data not shown). Assuming the coil was heated to its terminal temperature as defined by equation (4) then cooling upon deactivation of the power supply was modelled as

$$T(t) = \frac{U^2}{hAR}\mathrm{e}^{-\alpha t} + T_\mathrm{a}, \tag{5}$$

where $\alpha = 0.14$ was found via regression and $t = 0$ represents the point at which the power was cut. From equation (4) it follows that to obtain the NiTi's fully austenite temperature of 70 °C would require application of 1 V over 12 s, and the full prototype comprising 6 strings of 6 coils connected in parallel would require 6 V; though in practice this value was slightly lower due to the linkage chassis providing a degree of thermal insulation to the coils, reducing the value of h.

2.4. Simulation

It is the forces between separate links that dominate the mechanics and determine the final curvature of the fabric. To model this we used a rigid multi-body physics engine, which permits efficient calculations of the mechanical collisions and rotations between mechanically separate links, allowing us to scale up the simulations to model whole fabrics with hundreds of links [14, 15]. Multi-body physics engines employ a system of differential equations to relate the time derivative to the positions and velocities of a many body system and to balance the force equation that incorporates inertia, gravity and constraints such as friction [15, 16]. The validity of using this method assumes that the forces acting on the fabric are low enough that each linkage itself is not plastically deformed and that the elastic forces do not change the link geometries. In common with many dynamic and actively controlled robotic systems, these conditions are met in our material. The Bullet physics engine [15, 17] was selected for running our rigid body simulations due to its efficient collision detection for large sets of objects, its ability to capture friction, its capacity to constrain objects via a bespoke actuator model, and its ability to capture hysteresis effects.

The linkage design shown in figure 2(a) was modelled as a set of connected cuboid and cylinder primitives to improve stability and performance of the engine, which is typically not well suited for non-convex structures such as the topologically annular linkage. The two halves of the chassis were connected with pairs of tensile and compressive spring constraints to simulate the physical prototype, where the tensile spring constant k was set from equations (2)–(5). The number of iterations for Bullet's Projected Gauss Seidel [17] sequential impulse constraint solver was set to 10 000 to maximise the accuracy of the simulation over the large number of constraints involved. The masses of the simulated linkages were set to 7.3 g in accordance with the measured values. Coefficient of restitution was set to 0 as the SLA resin was found to exhibit negligible bounce, whilst coefficient of dynamic friction was set to 0.73.

2.5. Validation

The assembled prototype was connected to a 320 W power supply and tethered to a flat surface by the first two rows of linkages (figure 2(b)). 6 V was supplied, transforming the structure to full rigidity, and maintained for 12 s after which power was cut and the structure allowed to return to the flexible state. The same scenario was simulated in Bullet Physics, using equations (2)–(5) to set the effective spring constant of the NiTi springs in accordance with the input voltage profile. The simulation was then repeated without the NiTi model, where the spring constants were instantaneously set to their maximum and minimum values when the power was activated and deactivated.

To compare the results of the model and experiment, green circular markers were applied to the extremities of each of the linkages along one side of the physical model, while a video camera recorded activity in the y/z plane. The twelve markers were then extracted from the resulting video clip through colour thresholding and contour detection was applied to obtain the location of each marker's centroid. Markers were then manually assigned to pairs representing each of the six linkages being tracked, and the centres of each linkage were then used to compute the fabric's κ_max across the time domain.

An additional experiment was conducted to assess the linear contraction of the fabric, in which the prototype was suspended vertically through tethering the first row of linkages. The sample was then activated through application of

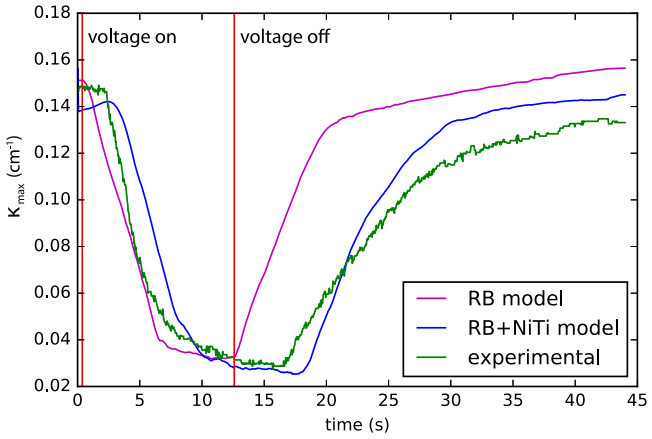

Figure 3. Flexibility of the active fabric over time in the observed (green) and simulated scenarios with (blue) and without (magenta) the NiTi heating model. Voltage was applied at 0.37 s and removed at 12.6 s indicated on figure by red vertical lines.

6 V and the total length of the fabric, measured from the base cylinders of the outer and inner most rows sharing common orientation, was recorded before, during and after activation.

3. Results and discussion

Upon application of the voltage, the individual links contract under actuation, transforming continuously from a curved drape profile to a rigid cantilever. In all cases the transformation was reversible, with the fabric regaining its flexibility when the power was cut. Figure 3 shows the maximum recorded curvature, as defined by equation (1), across the experimental (green) and simulated (blue with NiTi model and magenta without) fabrics over time. Noise in the experimental data is due to the stochastic contour finding algorithm used to track the markers, which was sensitive to changes in lighting exposure. The fully flexible and fully rigid states of the physical prototype are shown with the markers removed in figures 2(b) and (c). A video of the experiments is included as supplementary video 1 is available online at stacks.iop.org/SMS/26/08LT02/mmedia, and a video of the simulations is shown in supplementary video 2. The fabric was observed to undergo a linear contraction upon actuation during the experiment in which the sample was suspended vertically. At 0 V the prototype was measured to have total length 13.2 cm, whilst at 6 V the sample contracted to 11.5 cm equivalent to a linear strain of 12.9%. The change in length was reversible.

The good correspondence between the physical and computational results demonstrates that our method of using a rigid body physics engine coupled with analytical models of actuator performance proves to be a suitable way to explore the properties and devise control systems for active chainmail fabrics. The reduction in κ_{max} upon actuation, and its subsequent restoration as the NiTi coils cooled, indicates that this is a useful metric for quantifying flexibility in this particular case. Within the experimental data (green), delays can be observed between the power being applied and cut, and the resulting changes to the fabric's flexibility. These occurred due to the NiTi coils requiring time to heat and cool to within their critical temperature range (30 °C–70 °C), and were not captured by the purely rigid-body model (magenta). Hence we conclude that while the rigid-body system employed here is suitable for approximating the mechanical behaviour of chainmail fabrics in general, the dynamics of the active fabric could only be fully captured by our hybrid model (blue).

The use of SMAs means that the fabric's transition is a highly hysteretic process, largely due to the hysteresis inherent to NiTi actuators, and that even after several minutes (not shown) the prototype maintained a small residual κ_{max} following curtailment of actuation. We believe this is due to frictional forces occurring at the interface between linkages, and we found that once the restitution had plateaued the fabric could be manually manipulated back to its initial state with little resistance. It is possible that the wires connecting each of the linkages to the power source imposed an additional rigidity upon the fabric.

SMAs were used due to their availability in a miniature form that could be incorporated within the link geometry to control design parameters. Potential applications for our actuating fabrics could be found in morphing aerofoils as described in [5] and as a mechanism underlying active vibration absorbing systems. NiTi is currently used for many medical and orthodontic devices such as orthodontic wires, footwear and cardiac stents. It is an unsuitable actuator for many other applications due to issues of temperature control, hysteresis and thermal fatigue. However if the system were able to be miniaturised and the NiTi replaced with alternative actuators (see Hines *et al* [18] for an extensive review of the current state-of-the-art here) the approach could be used for many soft-robotic applications: potential uses include electroactive fabrics for load-bearing activities, dynamically reconfigurable orthoses and splints, and stiffening garments for preventing injury.

Both the physical and computational models show that the possibilities for actuated chainmail fabrics are mechanically rich. Whilst the structure investigated here was designed to have flexibility in only one axis, the methodology is general and can be applied to designs with parametric flexibility across three dimensions, although a different metric to our κ_{max} would be preferable in some such scenarios. Our use of the chainmail architecture allows for greater variation in flexibility than the laminate approach of Henry and McKnight [8], whilst keeping actuator strains comparably small.

4. Conclusions

We have developed a method for producing and analysing active chainmail fabrics with programmable flexibility. Through use of a rigid body physics simulation combined with an analytical model the dynamics of such an active fabric were captured, producing a design tool that can be used to generate active fabrics with bespoke properties. Simulations of dynamic modulation of the linkage geometry showed that flexibility could be manipulated in real time through actuating elements, and a physical prototype was constructed using

NiTi to validate this. NiTi is an unsuitable actuator for many applications, however we believe our methodology for designing actuated fabrics transcends this practical issue.

Acknowledgments

This work was funded by the EPSRC (EP/K020323/1) and a EPSRC CoMPLEX PhD studentship. We are also grateful for Inspiration Award from the UCL Centre for Nature Inspired Engineering funded through the EPSRC (EP/K038656/1).

References

[1] Franklin-Wallis O 2016 Flexible fashion: this 3D-printed dress flows like fabric *Wired Magazine*
[2] Rus D and Tolley M T 2015 Design, fabrication and control of soft robots *Nature* **521** 467–75
[3] Huh T M, Park Y-J and Cho K-J 2012 Design and analysis of a stiffness adjustable structure using an endoskeleton *Int. J. Precis. Eng. Manuf.* **13** 1255–8
[4] Long J H and Nipper K S 1996 The importance of body stiffness in undulatory propulsion *Am. Zoologist* **36** 678–94
[5] Thill C, Etches J A, Bond I P, Potter K D and Weaver P M 2008 Morphing skins *Aeronaut. J.* **112** 117–39
[6] Engel J and Liu C 2007 Creation of a metallic micromachined chain mail fabric *J. Micromech. Microeng.* **17** 551
[7] Rudykh S, Ortiz C and Boyce M C 2015 Flexibility and protection by design: imbricated hybrid microstructures of bio-inspired armor *Soft Matter* **11** 2547–54
[8] Henry C and Mcknight G 2006 Cellular variable stiffness materials for ultra-large reversible deformations in reconfigurable structures *Proc. SPIE* **6170** 536–47
[9] Otsuka K and Ren X 2005 Physical metallurgy of Ti–Ni-based shape memory alloys *Prog. Mater. Sci.* **50** 511–678
[10] Holschuh B, Obropta E and Newman D 2015 Low spring index NiTi coil actuators for use in active compression garments *IEEE/ASME Trans. Mechatronics* **20** 1264–77
[11] Chluba C, Ge W, Lima de Miranda R, Strobel J, Kienle L, Quandt E and Wuttig M 2015 Shape memory alloys. Ultralow-fatigue shape memory alloy films *Science* **29** 1004–7
[12] Smith C S 1959 Methods of making chain mail (14th to 18th centuries): a metallographic note *Technol. Cult.* **1** 60–7
[13] Song H, Kubica E and Gorbet R 1959 Resistance modelling of sma wire actuators *International Workshop Smart Materials Structures and NDT in Aerospace* 1 pp 2–4
[14] Trinkle J C, Pang J-S, Sudarsky S and Lo G 1997 On dynamic multi-rigid-body contact problems with coulomb friction *J. Appl. Math. Mech.* **4** 267–79
[15] Featherstone R 2008 *Rigid Body Dynamics Algorithms* (Berlin: Springer)
[16] Mazhara H, Osswaldb T and Negruta D 2016 On the use of computational multi-body dynamics analysis in sls-based 3D printing *Additive Manuf.* **12** 291–5
[17] Coumans E 2013 Open source: bulletphysics.org, Bullet Physics Library 15.
[18] Hines F, Petersen L K, Lum G Z and Sitti M 2017 Soft actuators for small-scale robotics *Adv. Mater.* **29** 1521–4095